Applied Physics Letters

Magnetic and magnetocaloric properties of layered van der Waals $CrCl_3$

Cite as: Appl. Phys. Lett. **117**, 092405 (2020); https://doi.org/10.1063/5.0019985
Submitted: 30 June 2020 . Accepted: 17 August 2020 . Published Online: 01 September 2020

Suchanda Mondal, A. Midya, Manju Mishra Patidar, V. Ganesan, and Prabhat Mandal

Applied Physics Letters ARTICLE scitation.org/journal/apl

Magnetic and magnetocaloric properties of layered van der Waals $CrCl_3$

Cite as: Appl. Phys. Lett. **117**, 092405 (2020); doi: 10.1063/5.0019985
Submitted: 30 June 2020 · Accepted: 17 August 2020 ·
Published Online: 1 September 2020

Suchanda Mondal,[1] A. Midya,[2] Manju Mishra Patidar,[3] V. Ganesan,[3] and Prabhat Mandal[1,a)]

AFFILIATIONS

[1]Saha Institute of Nuclear Physics, HBNI, 1/AF Bidhannagar, Calcutta 700 064, India
[2]Department of Physics, City College, 102/1, Raja Rammohan Sarani, Calcutta 700 009, India
[3]UGC-DAE Consortium for Scientific Research, University Campus, Khandwa Road, Indore 452 001, India

[a)]Author to whom correspondence should be addressed: prabhat.mandal@saha.ac.in

ABSTRACT

We have investigated the magnetic and magnetocaloric properties of van der Waals (vdW) layered $CrCl_3$ from magnetization and heat capacity measurements. $CrCl_3$ exhibits complicated magnetic properties due to the strong competition between the ferromagnetic and antiferromagnetic interactions: a ferromagnetic ordering around 17 K followed by an antiferromagnetic ordering at 14.3 K. A large magnetic entropy change ($-\Delta S_M$) of 19 J kg^{-1} K^{-1}, an adiabatic temperature change (ΔT_{ad}) of 6.2 K, and a relative cooling power of 600 J kg^{-1} are observed for a field change of 7 T near the transition temperature, and the mechanical efficiency (η_m) at 18 K and 0–3 T is 1.17. These values of magnetocaloric parameters are significantly larger than those for CrI_3 and other layered vdW systems. The scaling analysis shows that all the rescaled $\Delta S_M(T, H)$ data collapse into a single curve, which indicates the second order nature of magnetic phase transition. The above results suggest that environmentally friendly $CrCl_3$ can be a phenomenal alternative to very expensive rare-earth material for the magnetic refrigeration for liquefaction of hydrogen.

Refrigeration is the process of artificially cooling down a system below its ambient temperature, which has a great advantage not only for domestic purposes but also largely for commercial use such as industrial freezers, cryogenics, and the fuel industry. But the ever increasing demand of refrigeration causes a chronic effect on our environment as synthetic refrigerants mostly based on chlorofluorocarbon, hydrofluorocarbon, and hydrochlorofluorocarbon deplete the ozone layer, the shield against ultraviolet radiation. Magnetic refrigeration, an environmentally friendly cooling alternative to gaseous refrigeration, can achieve low temperature based on the magnetocaloric effect. In this process, the change in magnetic entropy determines the adiabatic temperature change of the material under the variation of the magnetic field. Using adiabatic demagnetization, one can reach ultra-low temperature, which has implicit usage in spacecraft, but it faces major challenges due to thermal and magnetic hysteresis.

Layered van der Waals (vdW) materials have attracted immense interest due to their remarkable physical properties and potential applications in microelectronics, spintronics, and optoelectronic devices.[1,2] Graphene and transition metal dichalcogenides are widely studied layered materials with adjacent layers bonded via weak vdW force having enormous applications in nanoelectronics and energy devices.[3,4] However, the absence of intrinsic magnetism in the 2D limit restricts their usage in spintronic devices. Recently, some layered vdW materials such as CrX_3 (X =Cl, Br, I), $Cr_2X_2Te_6$ (X =Ge, Si), Fe_3GeTe_2, and VI_3 have attracted tremendous interest because they retain intrinsic magnetism down to the monolayer or bilayer limit, which facilitates them in spin/valley electronics, vdW heterostructures, magnetoelectronics, and magneto-optics.[5–10] CrI_3, a member of the chromium trihalide family, shows long range ferromagnetism even at the monolayer limit and further shows bilayer antiferromagnetism, which is a promising candidate for low-dimensional spintronics as well as in fundamental physics[5,11] and $CrBr_3$; another ferromagnetic member of this family[11] retains ferromagnetism down to the monolayer.

In contrast, bulk $CrCl_3$ shows intralayer ferromagnetism with antiferromagnetic interaction between consecutive layers having a Neel temperature of $T_N = 14$ K with comparatively weak anisotropy.[12] In typical antiferromagnets, the magnetic moments are ordered, but the neighboring moments align along the opposite direction, resulting net zero magnetization (M). So in antiferromagnets, the stray current is zero. They have fascinating applications in spintronics, in which the spin–orbit torque can be controlled by the application of the electric

field.[13] CrI_3 has strong anisotropy and exhibits small anisotropic magnetic entropy changes ($-\Delta S_M$) as compared to conventional rare earth magnetocaloric materials.[14]

From extensive magnetic and thermal measurements, we report magnetic entropy changes along with the adiabatic temperature change (ΔT_{ad}) for $CrCl_3$ single crystals. The coefficient of performance (COP), η, which determines the energy efficiency of a refrigerator is also estimated to be very high, 1.17 for a field change of 0–3 T at 18 K. These evaluations of the magnetocaloric effect (MCE) refer to moderately large values of $-\Delta S_M$, ΔT_{ad}, and η, which suggest that $CrCl_3$ can be a magnificent alternative to rare earth material as a magnetic refrigerant near liquid hydrogen temperature in the commercial sector due to the high cost and less availability of the later corresponding to their comparable efficiencies.

$CrCl_3$ single crystals were grown by the chemical vapor transport method by recrystallizing $CrCl_3$ (99.995%, Alfa Aesar). Anhydrous $CrCl_3$ was sealed in an evacuated quartz tube and placed in a gradient furnace with a hot end at 700 °C and a cold end at 550 °C for a period of seven days. Thin violet colored plate-like crystals were collected from the cold end of the tube. The crystals were freshly cleaved before characterization and measurements. The structural analysis is carried out using a high-resolution Rigaku, TTRAX III (Cu-Kα radiation) x-ray diffractometer. The x-ray diffraction pattern from the surface of a cleaved thin single crystal of $CrCl_3$ corresponds to (0 0 l) peaks, confirming that the flat surface is perpendicular to the c axis with an interlayer spacing of 5.8086 Å (see the supplementary material). Magnetization and heat capacity measurements were performed using a physical property measurement system (PPMS, Quantum Design). The heat capacity was measured down to 2 K by the relaxation technique.

Figure 1(a) shows the temperature dependence of magnetization below 75 K with the $H||ab$ plane and the $H||c$ axis at 500 Oe and 1 kOe. Magnetization is comparatively smaller for the field along the c axis. Measurements are performed for both ZFC and FC conditions, but the data for the ZFC condition are shown for clarity. No significant difference between ZFC and FC data is observed. M increases sharply below 20 K, indicating the onset of ferromagnetic ordering. At low fields, M shows a cusp at 14 K due to antiferromagnetic ordering associated with antiparallel alignment of moments between two consecutive layers.[12,15] For further understanding of the magnetic ground state, inverse susceptibility (χ^{-1}) as a function of temperature is plotted in Fig. 1(a). χ^{-1} shows a nearly linear dependence on T both above and below the structural transition $T_S \approx 240$ K. In the temperature range of 250–380 K, susceptibility (χ) follows the Curie–Weiss law, $\chi = C/(T-\theta)$, with an effective paramagnetic moment of $\mu_{eff} = 3.72\ \mu_B/Cr^{3+}$ and a Weiss temperature of $\theta = 57.65$ K and a linear fit to the plot in the temperature range of 100–185 K gives $\mu_{eff} = 4.06\ \mu_B/Cr^{3+}$ and $\theta = 35.43$ K. The observed value of μ_{eff} is close to the theoretical spin-only moment ($S = 3/2$). μ_{eff} is close to the value reported earlier, whereas θ derived from $\chi^{-1}(T)$ above T_S is higher than the value in the previous report.[12] The positive value of Weiss temperature suggests that ferromagnetic interaction is of dominating nature in the paramagnetic state. In order to understand the effect of the magnetic field on the ground state, the isothermal magnetization for the $H||ab$ plane at 2 K is shown in the inset of Fig. 1(a). $M(H)$ shows negligible hysteresis. As the field increases, M increases sharply and tends to saturate at a field less than 3 kOe. This field is sufficient to completely orient the magnetic moments from the antiferromagnetic state to a field-induced spin-flip ferromagnetic state.[12,16] At 2 K and 5 T, the observed value of $M = 2.9\ \mu_B/Cr^{3+}$ corresponds to spin only moment of Cr. For insight into the magnetic phase transition in $CrCl_3$, M^2 as a function of H/M ($H||ab$) is plotted in Fig. 1(b) to construct the Arrott plot around the onset of the magnetic ordering. The nature of the Arrott plot for the present system differs significantly from the critical behavior of the conventional ferromagnet. The curvatures in the M^2 vs H/M isotherms in the low-field region are strongly temperature dependent. For $T > 17$ K, the isothermal curves mimic the Arrott plot of conventional ferromagnetic phase transition with magnetic fluctuations above T_C. The magnetic fluctuation above T_C in $CrCl_3$ is also reflected from the large Weiss temperature, which is about two times of T_C. Below $T = 17$ K, the nature of the curvature of M^2 vs H/M isotherms at low fields changes rapidly with decreasing temperature. The squared magnetization falls off rapidly as the field is decreased to zero for isotherms below 14 K. The deviation of the Arrott plot from that observed in a conventional ferromagnetic phase transition is consistent with the fact that the long-range magnetic order in $CrCl_3$ sets in at low temperatures in a two-step process.[12] Below the Weiss temperature, ferromagnetic correlation develops between the Cr spins lying in the ab-plane and becomes the strongest at around 17 K. However, the onset of the antiferromagnetic

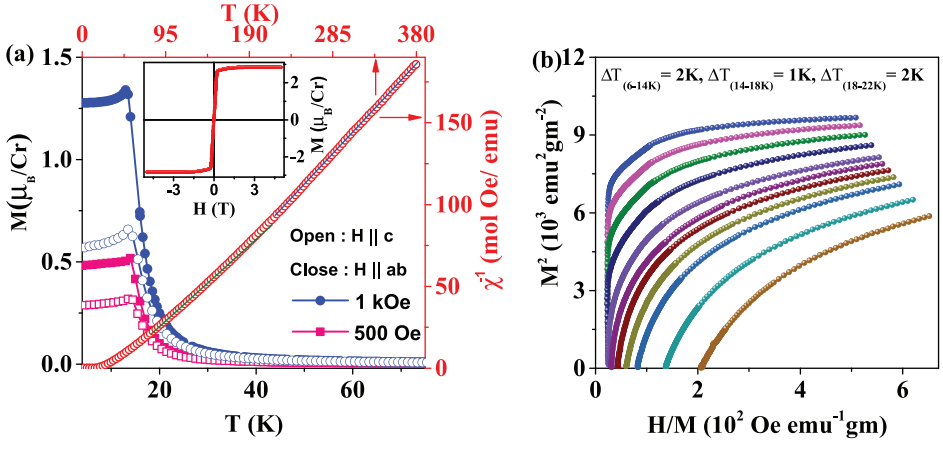

FIG. 1. (a) Magnetic moment vs temperature measured for the applied field both parallel and perpendicular to the plane. Temperature-dependent inverse susceptibility $\chi^{-1}(T)$ for $CrCl_3$ single crystals measured at a field of 1 kOe with the $H||ab$ plane; solid lines are the Curie–Weiss fit. Isothermal magnetization with the $H||ab$ plane at T = 2 K is shown in the inset. (b) The Arrott plot for $CrCl_3$.

correlations between the ferromagnetic *ab*-layers at about 14 K reinforces the system to enter a long-ranged antiferromagnetic ground state at low temperatures and breaks the time reversal symmetry. The universality class of the system is, thus, governed by the antiferromagnetic phase transition at $T_N = 14$ K, where the correlation length diverges rather than the transition to short-range ferromagnetic ordering at $T = 17$ K. The evolution of the true order parameter of the phase transition, i.e., the spontaneous magnetization with temperatures and T_C, cannot be determined from the extrapolation of the Arrott plot or modified Arrott plot isotherms at high fields to zero and from quadratic extrapolation of the Arrott plot to zero field as have been done in several systems.[17] However, the sub-lattice magnetization can be deduced from the neutron scattering experiments at different temperatures around 14 K to determine the true nature of the magnetic phase transition in $CrCl_3$.

$M(H)$ curves for the $H||ab$ plane and the $H||c$ axis are depicted in Figs. 2(a) and 2(b) after demagnetization correction as discussed in the earlier report.[12] At low temperature, $M(H)$ for the $H||c$ axis also saturates at fields less than 3 kOe. To test whether this material is suitable for magnetic refrigeration, magnetic entropy changes have been calculated as $\Delta S_M = \sum_i \left(\frac{M_{i+1}-M_i}{T_{i+1}-T_i}\right)\Delta H_i$, where M_{i+1} and M_i are the magnetic moments at temperatures T_{i+1} and T_i, respectively, with the change in magnetic field ΔH_i. $\Delta S_M(T)$ for the $H||ab$ plane and the $H||c$ axis is shown in Figs. 3(a) and 3(b), respectively. ΔS_M increases with increasing T and reaches maximum at T_C for low fields. As the applied field increases, the maximum value of ΔS_M (ΔS_M^{max}) increases and ΔS_M^{max} becomes 19.8 J kg^{-1} K^{-1} for $H||ab$ and 19.5 J kg^{-1} K^{-1} for $H||c$ at 7 T. Thus, ΔS_M is almost isotropic in $CrCl_3$. The negative sign of ΔS_M indicates the reduction of temperature when the magnetic field changes adiabatically.

For understanding the nature of the magnetic ground state and intrinsic magnetocaloric properties, heat capacity is measured as a function of temperature and field (Fig. 4). At zero field, C_P exhibits a sharp λ-like anomaly at 14 K, which diminishes with the field and disappears above $H = 2$ kOe. The λ-like anomaly is followed by a broad facet centered at T_C. With the application of the field, this facet further broadens and shifts toward higher temperature. The $C_P(T)$ curve fits well with the combined Debye plus Einstein model of lattice heat capacity (C_L) over a wide temperature range as shown in Fig. 4(a) (see the supplementary material). By subtracting the lattice contribution from total heat capacity, the magnetic contribution (C_m) is determined as depicted in Fig. 4(b). The entropy estimated by integrating C_m/T is about 10.2 J mol^{-1} K^{-1} at zero field, which is close to the theoretical value of $R\ln(2S+1) = 11.5$ J mol^{-1} K^{-1} as shown in the inset of Fig. 4(a). To check whether the magnetic entropy change from the $M(H)$ plot is consistent or not, $-\Delta S_M$ is calculated from heat capacity

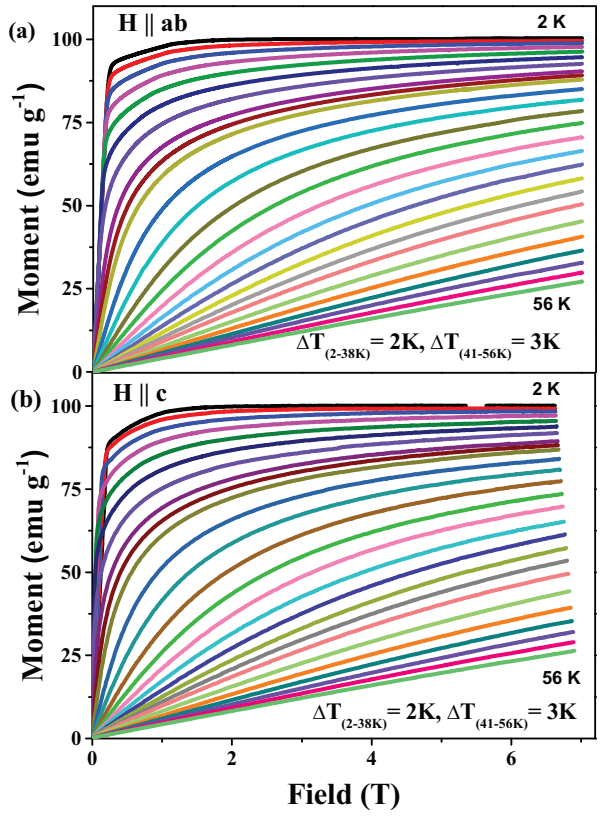

FIG. 2. Isothermal magnetization curves for the field applied along (a) $H||ab$ plane and (b) $H||c$ axis.

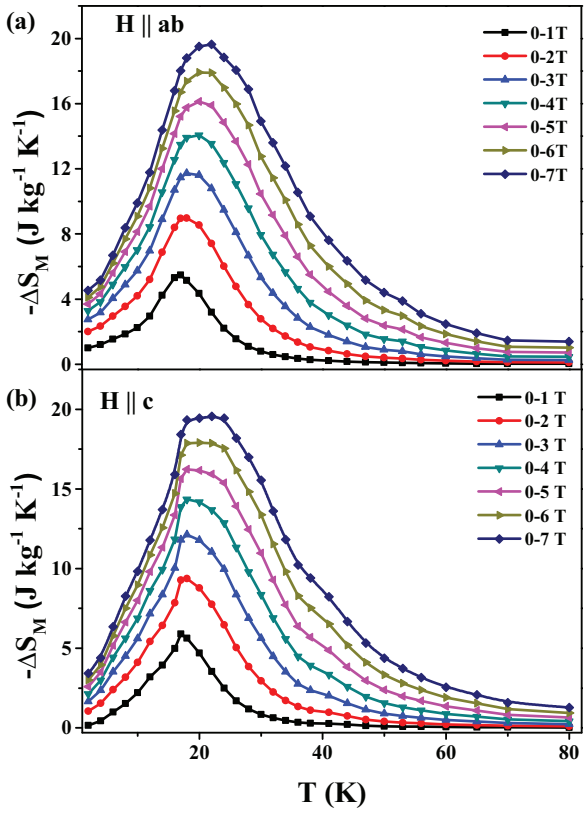

FIG. 3. (a) Temperature variation of $-\Delta S_M$ calculated from magnetization data for the $H||ab$ plane. (b) Temperature variation of $-\Delta S_M$ calculated from magnetization data for the $H||c$ axis.

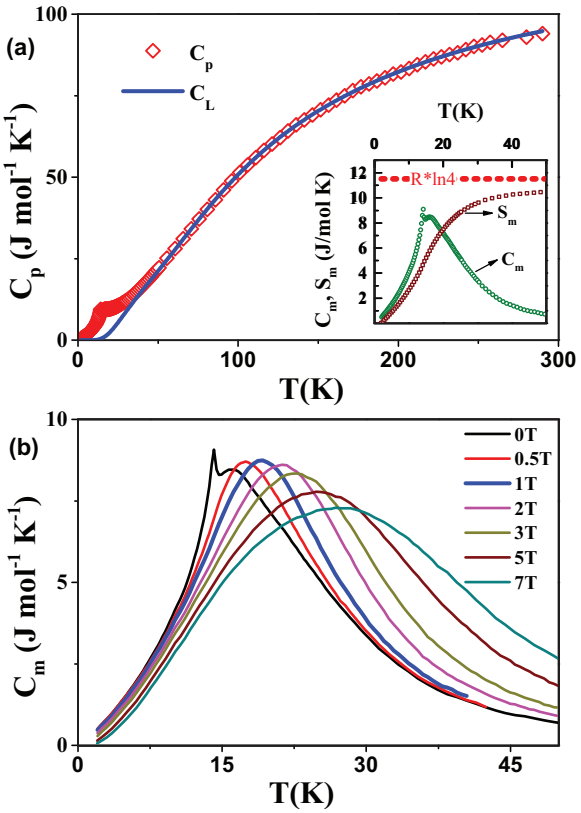

FIG. 4. (a) The zero field heat capacity data and combined Debye–Einstein fit (solid line). Estimated magnetic entropy and magnetic heat capacity are shown in the inset. (b) Temperature dependence of magnetic heat capacity for different fields.

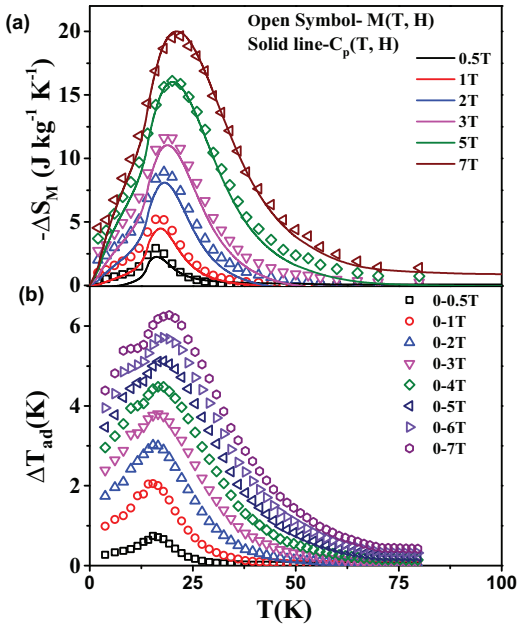

FIG. 5. (a) Temperature variation of $-\Delta S_M$ at different fields calculated from the heat capacity data. (b) Temperature dependence of adiabatic temperature change ΔT_{ad} at different fields.

data as shown in Fig. 5(a). This plot reveals that both the values of ΔS_M are close to each other. A small difference between these two may be due to the overestimation of lattice contribution. The adiabatic temperature change $\Delta T_{ad} = T_i - T_f$ is defined as the temperature change of the system from initial temperature T_i $(H = 0)$ to final temperature T_f $(H \neq 0)$ in an isentropic process caused by the intrinsic magnetocaloric effect. We have calculated ΔT_{ad} from zero field heat capacity and ΔS_M data. $\Delta T_{ad}(T)$ at different fields is shown in Fig. 5(b). With the increase in the field, the maximum value of ΔT_{ad} increases and becomes 6.8 K for 0–7 T. Both ΔT_{ad} and ΔS_M for bulk $CrCl_3$ single crystals are quite large compared to those reported for other vdW systems (Table I).

A phenomenological curve for ΔS_M for different applied magnetic fields has been proposed by Franco *et al.* as a way to determine the order of magnetic phase transition.[19] In this method, the parameters related to $\Delta S_M(T)$ curves follow a series of power laws dependent on the field: $|\Delta S_M^{max}| \propto H^n$, $\delta T_{FWHM} \propto H^b$, and RCP $\propto H^c$, where δT_{FWHM} is the full-width at half maximum and RCP is the relative cooling power.[19,20] For temperature well above T_C, the value of n for all applied fields tends to 2, which points toward the second order nature of phase transition[21] (for plots and analysis, see the supplementary material). From scaling analysis, all the $\Delta S_M(T, H)$ plots collapse into a single curve for the $H||ab$ plane, which reveals that the corresponding phase transition is second order in nature[24] (for details, see the supplementary material). For understanding the nature of magnetic interaction in $CrCl_3$, a detailed neutron scattering study of this layered material can be very interesting.

In conclusion, the calculated values of ΔS_M, ΔT_{ad}, and RCP are large compared to those of CrI_3 and other layered vdW systems. $-\Delta S_M$ values for two directions of the applied field with the $H||ab$ plane and the $H||c$ axis are almost the same, which is attributed to the very weak anisotropy in $CrCl_3$. Our result suggests that single crystal $CrCl_3$ can have potential application as a magnetic refrigerant at liquid hydrogen temperature.

Note that after submitting this manuscript we came to know about the investigation of the magnetocaloric effect in $CrCl_3$ single crystals by Liu *et al.*,[25] which does not explore the isotropic nature of the MCE, considering the demagnetization correction. Also, they have not calculated magnetic entropy changes and adiabatic temperature changes from the heat capacity measurement.

TABLE I. Parameters for layered vdW refrigerant materials at liquid-hydrogen temperature for a field change of 0–2 T.

vdW systems	$-\Delta S_M^{max}$ (J kg^{-1} K^{-1})	T^{max} (K)	δT_{FWHM} (K)	RCP (J kg^{-1})	References
$CrCl_3$	8.97	18	16.09	144.35	This work
CrI_3	2.4	60	18.8	45	14
$Fe_{3-x}GeTe_2$	0.8	155	50	40	18
$Cr_2Ge_2Te_6$	2	68	21	38	22
VI_3	1.9	50	8.9	17	23

See the supplementary material for detailed analysis and plots for determination of order of transition and efficiency.

The authors are very much thankful to Dr. Nazir Khan for his valuable assistance in the revised manuscript. The authors also would like to thank A. Paul for his help during the measurements. V.G. contributed to this work while in service, acknowledges UGC-DAE CSR for LTHM facilities, and would like to thank Senior Cryogenic Engineer Er. P. Saravanan.

DATA AVAILABILITY

The data that support the findings of this study are available from the corresponding author upon reasonable request.

REFERENCES

[1]J. Schaibley, H. Yu, G. Clark, P. Rivera, J. S. Ross, K. L. Seyler, W. Yao, and X. Xu, Nat. Rev. Mater. **1**, 16055 (2016).
[2]E. Pomerantseva and Y. Gogotsi, Nat. Energy **2**, 17089 (2017).
[3]R. Raccichini, A. Varzi, S. Passerini, and B. Scrosati, Nat. Mater. **14**, 271 (2015).
[4]S. Manzeli, D. Ovchinnikov, D. Pasquier, O. V. Yazyev, and A. Kis, Nat. Rev. Mater. **2**, 17033 (2017).
[5]B. Huang, G. Clark, E. Navarro-Moratalla, D. R. Klein, R. Cheng, K. L. Seyler, D. Zhong, E. Schmidgall, M. A. McGuire, D. H. Cobden, W. Yao, D. Xiao, P. Jarillo-Herrero, and X. Xu, Nature **546**, 270 (2017).
[6]C. Gong, L. Li, Z. Li, H. Ji, A. Stern, Y. Xia, T. Cao, W. Bao, C. Wang, Y. Wang, Z. Q. Qiu, R. J. Cava, S. G. Louie, J. Xia, and X. Zhang, Nature **546**, 265 (2017).
[7]C. Tan, J. Lee, S.-G. Jung, T. Park, S. Albarakati, J. Partridge, M. R. Field, D. G. McCulloch, L. Wang, and C. Lee, Nat. Commun. **9**, 1554 (2018).
[8]T. Kong, K. Stolze, E. I. Timmons, J. Tao, D. Ni, S. Guo, Z. Yang, R. Prozorov, and R. J. Cava, Adv. Mater. **31**, 1808074 (2019).
[9]M. Gibertini, M. Koperski, A. F. Morpurgo, and K. S. Novoselov, Nat. Nanotechnol. **14**, 408 (2019).
[10]H. Li, S. Ruan, and Y.-J. Zeng, Adv. Mater. **31**, 1900065 (2019).
[11]M. A. McGuire, H. Dixit, V. R. Cooper, and B. C. Sales, Chem. Mater. **27**, 612 (2015).
[12]M. A. McGuire, G. Clark, S. KC, W. M. Chance, G. E. Jellison, Jr., V. R. Cooper, X. Xu, and B. C. Sales, Phys. Rev. Mater. **1**, 014001 (2017).
[13]V. Baltz, A. Manchon, M. Tsoi, T. Moriyama, T. Ono, and Y. Tserkovnyak, Rev. Mod. Phys. **90**, 015005 (2018).
[14]Y. Liu and C. Petrovic, Phys. Rev. B **97**, 174418 (2018).
[15]B. Kuhlow, Phys. Status Solidi A **72**, 161 (1982).
[16]J. W. Cable, M. K. Wilkinson, and E. O. Wollan, J. Phys. Chem. Solids **19**, 29 (1961).
[17]E. M. Clements, R. Das, L. Li, P. J. Lampen-Kelley, M.-H. Phan, V. Keppens, D. Mandrus, and H. Srikanth, Sci. Rep. **7**, 6545 (2017).
[18]Y. Liu, J. Li, J. Tao, Y. Zhu, and C. Petrovic, Sci. Rep. **9**, 13233 (2019).
[19]V. Franco, A. Conde, J. M. Romero-Enrique, and J. S. Blázquez, J. Phys.: Condens. Matter **20**, 285207 (2008).
[20]V. Franco, J. S. Blázquez, and A. Conde, Appl. Phys. Lett. **89**, 222512 (2006).
[21]J. Y. Law, V. Franco, L. M. Moreno-Ramírez, A. Conde, D. Y. Karpenkov, I. Radulov, K. P. Skokov, and O. Gutfleisch, Nat. Mater. **9**(1), 2680 (2018).
[22]W. Liu, Y. Dai, Y.-E. Yang, J. Fan, L. Pi, L. Zhang, and Y. Zhang, Phys. Rev. B **98**, 214420 (2018).
[23]J. Yan, X. Luo, F. C. Chen, J. J. Gao, Z. Z. Jiang, G. C. Zhao, Y. Sun, H. Y. Lv, S. J. Tian, Q. W. Yin, H. C. Lei, W. J. Lu, P. Tong, W. H. Song, X. B. Zhu, and Y. P. Sun, Phys. Rev. B **100**, 094402 (2019).
[24]C. Romero-Muñiz, R. Tamura, S. Tanaka, and V. Franco, Phys. Rev. B **94**, 134401 (2016).
[25]Y. Liu and C. Petrovic, Phys. Rev. B **102**, 014424 (2020).